



Aldaikh, H., Alexander, N., Ibraim, E., & knappett, J. (2016). Shake Table Testing of the Dynamic Interaction between Two and Three Adjacent Buildings (SSSI). *Soil Dynamics and Earthquake Engineering*, 89, 219-232.  
<https://doi.org/10.1016/j.soildyn.2016.08.012>

Peer reviewed version

License (if available):  
CC BY-NC-ND

Link to published version (if available):  
[10.1016/j.soildyn.2016.08.012](https://doi.org/10.1016/j.soildyn.2016.08.012)

[Link to publication record in Explore Bristol Research](#)  
PDF-document

This is the accepted author manuscript (AAM). The final published version (version of record) is available online via Elsevier at <http://dx.doi.org/10.1016/j.soildyn.2016.08.012>. Please refer to any applicable terms of use of the publisher.

## University of Bristol - Explore Bristol Research

### General rights

This document is made available in accordance with publisher policies. Please cite only the published version using the reference above. Full terms of use are available:  
<http://www.bristol.ac.uk/red/research-policy/pure/user-guides/ebr-terms/>

2

## 3 **Shake Table Testing of the Dynamic Interaction between Two and**

## 4 **Three Adjacent Buildings (SSSI)**

5

6 **Hesham Aldaikh<sup>a,c\*</sup>, Nicholas A. Alexander<sup>b</sup>, Erdin Ibraim<sup>b</sup> and Jonathan Knappett<sup>c</sup>**

7 <sup>a</sup>Department of Engineering, University of Cambridge. Cambridge CB2 1PZ, UK. *Formerly University of Bristol, UK.*  
8 (hsha2@cam.ac.uk)

9 <sup>b</sup> Department of Civil Engineering, University of Bristol. Bristol, BS8 1TR, UK (nick.alexander@bristol.ac.uk and  
10 erdin.ibraim@bristol.ac.uk)

11 <sup>c</sup> Division of Civil Engineering, University of Dundee. Dundee DD1 4HN, UK (j.a.knappett@dundee.ac.uk)

### 12 **Abstract**

13 The dynamic interaction of adjacent buildings in cities and urban areas through the soil medium is inevitable.  
14 This fact has been confirmed by various analytical and numerical studies. However, very little research is  
15 available on the physical modelling of the Structure-Soil-Structure Interaction (SSSI) problem and its effect  
16 on the dynamics of adjacent structures. In this paper, a series of shaking table tests was conducted at the  
17 Earthquake and Large Structures Laboratory (EQUALS) at the University of Bristol to examine the effects of  
18 SSSI on the response of a model building when bordered by up to two other model buildings under dynamic  
19 excitation. The results indicated that depending on their height, the presence of one or two adjacent building  
20 could positively or negatively alter seismic power and peak acceleration responses of a building in comparison  
21 to when it is tested in isolation.

22

23 **Keywords:** Structure-Soil-Structure Interaction (SSSI), Physical Modelling, Shake Table, Seismic Response.

24

\*Corresponding author at: Cambridge Centre for Smart Infrastructure and Construction, Department of Engineering, University of  
Cambridge. Trumpington St. Cambridge CB2 1PZ.

email addresses: cexha@my.bristol.ac.uk  
hsha2@cam.ac.uk

## 1 Introduction

Interaction among adjacent buildings in cities and urban areas is considered one of the major unsolved problems in the field of earthquake engineering [1]. The phenomenon is mainly referred to as Structure-Soil-Structure Interaction (SSSI) and has been previously investigated although not nearly as extensively as the conventional Soil-Structure Interaction (SSI) problem. As a natural protraction, research techniques implemented in investigating SSSI are similar to those used in SSI analyses [2]. In fact, a real or complete SSI analysis must take into account the possible consideration of interaction with neighbouring structures [3].

Studies of SSSI have principally been focused on theoretical derivations and numerical simulations. Early imperative analytical studies, notably [4], [5], [6] and [7] have laid the cornerstone and led to a considerable understanding of the phenomenon. Interaction was found to be important in the low-frequency range associated with a resonance frequency of the complete SSSI system. The interaction effect was also found to be especially prominent if the structure of interest is smaller and lighter than its neighbours and that interaction between buildings of comparable sizes may cause the amplitude response to become large. Numerical studies are mainly based either on two or three dimensional finite element modelling (FEM) such as [8], [9], or the boundary element method (BEM) [10], [11] or hybrid FEM/BEM procedures [12], [13]. These studies have emphasized the scale of the problem and its importance for consideration in the dynamic analyses, including the identification of key factors that may control the degree of multi-structural interactions, for example: relative inertial and dynamic characteristics of adjacent buildings, separation building distances, soil type and the configuration of the buildings' plan arrangements.

The study in [14] analytically investigated the interaction of three different adjacent buildings utilising an equivalent linear model to approximately account for large shear strains in soil. It was found that the interaction could not be neglected if the buildings are spaced at a distance equal to half of the building base width. The reader may refer to the literature survey conducted in [2] for a more complete review on the history, status, research methods and future research trends of SSSI. Analytical studies in [15-18] employed simple discrete models and reduced the size of the interaction problem of two and three adjacent buildings to a meaningful set of characteristics of the structures, distance between them and soil type which allowed an insight into the effect of these parameters on SSSI.

The least implemented method applied to the SSSI problem is physical modelling. Some early experimental studies such as the ones conducted by [19] and [20] reasonably represented the major SSSI problem. However, some significant discrepancies in results were found compared to analytical solutions. It was argued that as tests were conducted over several months, realising similarity to previously conducted tests was difficult and change in moisture content may have resulted in gradual compaction of soil.

The study in [21] utilised shaking table model test results of dynamic interaction between two identical foundations made of aluminium resting on a silicon rubber ground model to calibrate 2D finite element and 3D boundary element models. The SSSI effect was found to be relatively small in terms of foundation

displacement and acceleration but more significant in terms of soil pressure. Experimental studies of SSSI have gained a rapid development in Japan. For example, the study in [22] conducted forced vibration field tests of two adjacent “mock-up” foundations and a third simple building model supported on piles in sandy soil. Numerical comparisons using a 3D thin layer soil model showed a good agreement with the experiment. It was concluded that large mass foundations have strong effects (frequency response amplification) on foundations of smaller mass in the natural frequency vicinity of the large mass foundation.

The Nuclear Power Engineering Corporation of Japan has conducted a series of experimentations on the Dynamic Cross Interaction problem in nuclear power plants [23-26]. The project consisted of field and laboratory tests. Different patterns were noticed in the Fourier Spectra of a single building compared to that after constructing an adjacent building, with attenuations in amplitude peaks. The study showed that the adjacency effect was stronger when the same type of building was closely adjacent in the direction of vibration. The project concluded that to obtain satisfactory results for precise seismic analysis SSSI effects cannot be neglected.

An experimental study in [27] conducted a 1:15 scale model shaking table tests on the interaction of two identical adjacent 12 storey cast-in-place reinforced concrete frames supported by pile foundations. The SSSI was found to have no influence on the frequency and characteristics of the vibration modes but depending on the magnitude of the input excitation, the peak acceleration of the superstructure either decreased or increased compared to that of SSI. Peak acceleration within the soil and peak contact pressure along the pile-soil interface was greater when compared to that of a single SSI system

Some recent experimental studies on the topic [28, 29] have studied the inelastic structural response of two adjacent steel moment-resisting frames in a geotechnical centrifuge subjected to strong ground shaking in either an in-plane or out of plane orientations. A physical restraining effect was observed when a shorter frame with shallow foundations was placed near to a taller frame (approximately 3 times taller) with a basement. This lead to increased base shear and moments compared to the isolated case. Kinematic interaction, conventionally neglected in engineering design, was found to have a significant effect on structural response and caused reductions in higher frequency content and foundation level amplitudes. A similar result was also found by [30], using centrifuge modelling of similar and highly dissimilar buildings on shallow foundations (but without basements), where structural response was shown to either increase or decrease depending on the relative configurations (dynamic properties) of pairs of adjacent structures. The numerical and experimental study by [31, 32] proposed a novel vibration control strategy based on the SSSI phenomenon to reduce structural vibrations of monopile structures due to seismic waves. The proposed structural system, termed “Vibrating Barrier”, was found to cause a reduction in the displacement response of structures by up to 44%.

More recently, Schwan et al [33] presented an experimental SSSI setup that comprised an idealized small-scale site-city model with groups of 5, 9, 19 and 37 identical anisotropic model structures arranged in resonance with an elastic layer on which surface they were adhered. The experimental results were validated against a theoretical city-impedance model (CIM) derived from a homogenization method and a numerical Boundary

Elements (BE) model. A split in the city layer resonant peak was noticed in comparison to the single peak without the presence of the city. Increases in response amplitudes and city resonance frequency evidenced that the denser the city the stronger the interaction effect which could be detected when the number of adjacent structures is as low as 5. This experimental study was conducted at the Earthquake and Large Structures Laboratory (EQUALS) at the University of Bristol and have inspired the choice of the materials used in the current experimental work.

Based on the discussion above, there is considerable scope for further parametric experimental studies to provide valuable insight into understanding the dynamic behaviour of multiple adjacent structures. The main aim of this test programme is to explore the effect of system dynamic parameters on coupled seismic structural responses. Extending from this aim one of the objectives is to explore the effect of structural height (and hence period) on response magnitudes. Another objective is to use the results from this experimental study to validate analytical discrete models previously presented in [17, 18]. In the current paper, we present new experimental and finite element results for the case of two and three adjacent buildings. A comparison between this 1g test and a centrifuge model, [30], is also presented.

The concept of the experimental investigation presented in this paper is to construct a linear elastic ‘plane strain’ physical model of Structure-Soil-Structure Interaction between up to three adjacent structures. In this system, scaled models of adjacent structures are placed upon a flexible base (i.e. a soil substitute) made of cellular Polyurethane foam while subjecting it to different ground motions conveyed via a shaking table. As the aim of the current study is to examine the SSSI problem within the linear response of buildings, the choice of the foam material instead of real soil is justified. Large amplitude dynamic excitation of granular soils on the shaking table can be challenging due to the soils nonlinear nature. Changes in the soil internal packing due to ground vibrations may lead to altering properties of subsequent tests, hence compromising repeatability. Soil (or soil substitute) in particular is aimed to be invariant during tests to enable the examination of different ground motions and building configurations under nominally identical initial conditions. In [33, 34] a block of the same foam material used in this study has proven to be a suitable soil representation for elasto-dynamic experimentation.

Hence, the scope of this experimental study is restricted by the following:

- i- Linear elasticity for both building models and soil substitute.
- ii- Interaction between up to three adjacent buildings
- iii- Building models have an identical plan area
- iv- Buildings can be of different heights
- v- Buildings are equispaced at a fixed distance from each other

The small-scale physical test programme reported herein has been carried out utilising the shaking table facility at EQUALS in the Earthquake Engineering Research Centre (EERC) at the University of Bristol.

## 2 Experiment

### 2.1 Scaling down of the problem (design of a 1g model)

In any small-scale experiment establishing parameter similitude laws between a prototype and an experimental model is the first step to undertake. For small scale shaking table testing, i.e. 1g conditions, maintaining this similitude while allowing testing repeatability could prove challenging. Studying and understanding the fundamental mechanics of the problem is one way of designing model tests and achieving the appropriate similitude, [35]. It has been shown in previous studies, such as Veletsos and Nair [36] and Bielak [37], that among the most important non-dimensional parameters that control the Soil-Structure Interaction effects are: *ratio of structure mass to the mass of soil*; *structure-to-soil stiffness ratio* and *structure-height-to-foundation-width ratio*. Previous analytical studies by the authors [17, 18] introduced a structure-soil-structure system in which each structure-soil system consists of a two degree of freedom. The Appendix contains the derivation of the equation of motion, equation (13), for such a system. This system is governed by three non-dimensional parameters, namely: (i) a mass ratio ( $\alpha$ , the ratio of soil-foundation mass to structure mass); (ii) a frequency ratio ( $\Omega$ , the ratio of the soil-foundation frequency parameter to the fixed base structural frequency). This can be consider as an alternative to using a stiffness ratio. (iii) an aspect ratio ( $\eta$ , the ratio of structure's height to the soil's area radius of gyration). Therefore, if these non-dimensional parameters are approximately the same in the prototype and the experimental models then a dynamic similitude is achieved for the given assumptions of the analysis.

The main structure prototype is based on a three storey reinforced concrete structure resting on a site of loose sand where it has been demonstrated that SSSI effects may result in significant interaction [17]. The prototype building has a height  $h=9.6$  m, an aspect ratio  $S_B = h/b_B \approx 3\eta$  (building height to width ratio) of 3, an average density  $\rho_B$  of  $600 \text{ kg/m}^3$  resting on a loose sand profile of density  $\rho_s=1300 \text{ kg/m}^3$ , having a Poisson's ratio  $\mu_s=0.3$  and a shear wave velocity  $V_s=150 \text{ m/s}$ , which corresponds to ground type D according to EC8 [38] or a site class E according to NEHRP provisions [39]. From [17] the prototype has a non-dimensional mass ratio  $\alpha$  as follows

Prototype: 
$$\alpha = \frac{m_2}{m_1} = \frac{\text{Soil-foundation mass}}{\text{Building mass}} = 0.35 \frac{\rho_s}{\rho_B} \frac{1}{S_B} = 0.25 \quad (1)$$

The fundamental angular frequency of the building prototype is taken as  $\omega_1 \approx 200/h_B = 20.8 \text{ rad/s}$  where  $h_B$  is the building height [m]. This formula is derived based on an empirical result suggested in the SEAOC Blue Book [40] for the natural period of a structure on a rigid foundation in seconds is  $N/10$  for  $N \leq 12$ , where  $N$  is the number of storeys for an average storey height of 3.2 m. It is worth noting that  $\Omega_f$  (which is the ratio of flexible-base fundamental natural frequency  $\omega_{f1}$  to fixed-based fundamental natural frequency  $\omega_1$ ) is

functionally related to only the three system parameters, namely  $\Omega$ ,  $\eta$  and  $\alpha$  (see equation (13) in the appendix); therefore  $\Omega_f$  we are not mathematically required match this parameter for dynamic similitude.

Using the definition in the Appendix (equation (10)), the soil-foundation frequency parameter  $\omega_2$  can be estimated using various empirical formulae discussed in [17] hence,

$$\text{Prototype: } \omega_2 = \sqrt{\frac{k_2}{m_2 r^2}} = \sqrt{\frac{0.5 G_s b_B^3 / (1 - \mu)}{(0.35 b_B^3 \rho_s)(0.33 b_B)^2}} = \sqrt{\frac{13.1 \times 10^6}{(1 - \mu_s) b_B^2}} \bar{V}_s = 224.95 \text{ rad/s} \quad (2)$$

where  $k_2$  is rotation soil spring [41],  $r = b_B/3$  is the radius of gyration of the soil-foundation mass,  $0.35 b_B^3$  is the volume of soil-foundation mass [42],  $G_s$  is the soil shear modulus,  $b_B$  is the width of the building foundation and  $\bar{V}_s$  is a normalised soil shear wave velocity (*viz.* the ratio of the soil shear wave velocity  $V_s = \sqrt{G_s / \rho_s}$  [m/s] to a reference shear wave velocity of 1000 m/s (which is notionally the value in a stiff soil). Hence the prototype non-dimensional frequency ratio is

$$\text{Prototype: } \Omega = \frac{\omega_2}{\omega_1} = 10.8 \quad (3)$$

## 2.2 Soil Substitute (Polyurethane Foam)

The Polyurethane foam block used is shown in Figure 1 and has dimensions of 1000x1000x750 mm<sup>3</sup>. In order to facilitate handling and clamping to the shaking table platform, a square wooden plate was firmly secured to the foam at its base with a contact adhesive, while its lateral sides were free of any constraints. During shaking the experimental model is positioned on the platform so that its principal axes are aligned with the driven axes of the shaking table. The elastic properties of the foam block are: elastic modulus  $E_f = 120 \text{ kN/m}^2$ ; Poisson's ratio  $\mu_f = 0.11$  and density  $\rho_f = 50 \text{ kg/m}^3$ , [34].

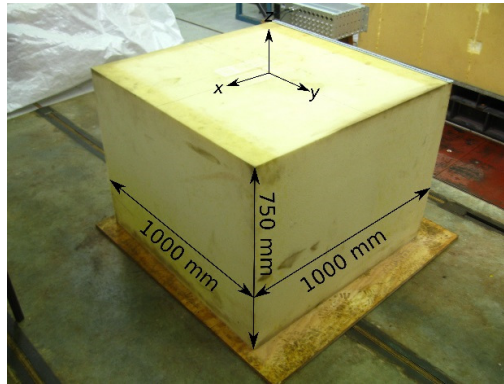
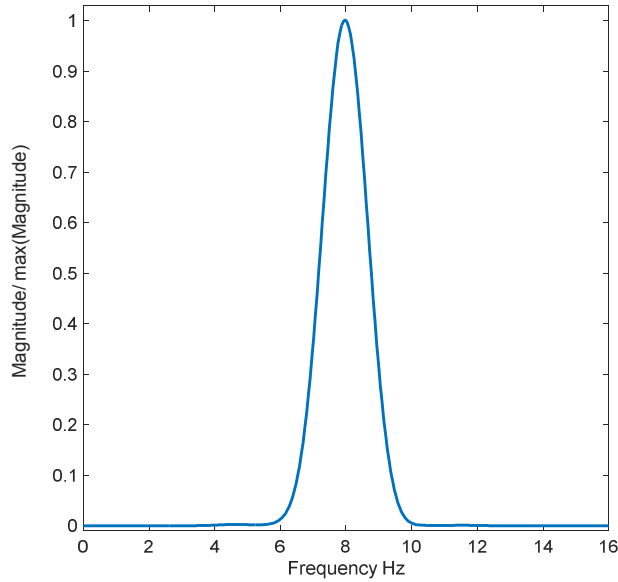


**Figure 1** Geometry of Polyurethane foam block

183

### 184 2.1.1 Dynamic Properties of foam block

185 The dynamic properties of the foam block were obtained by performing a free vibration test. The foam was  
 186 excited (i.e. hitting it on the top side with a steel rod) by a small amplitude arbitrary impulse in the horizontal,  
 187  $x$ , direction and allowed to vibrate freely. The power spectrum of the signal revealed a natural frequency of 8  
 188 Hz and a damping ratio of 4.3 % calculated using the half- power bandwidth method (Figure 2). The same  
 189 natural frequency was obtained in the  $y$  direction.



190

191

**Figure 2** Natural frequency of foam block.

### 192 2.3 Model Buildings

193 In accordance with the values of the mass and frequency ratios stated in Equations (2) and (4) the main  
 194 experimental building model was designed having the geometry shown in Figure 3 and is referred to as ‘B1’.  
 195 Assuming an added mass associated with the vibration of structure ( $m_f$ ) that is approximately equivalent to half  
 196 a cylinder (diameter of  $b_m$ ), [42], results in the following mass ratio for the experimental model

197 Model:

$$\alpha = \frac{m_2}{m_1} = \frac{m_f + m_c}{m_a + m_b} = 0.266 \quad (4)$$

198 where  $m_f=0.014$  kg,  $m_c=0.26$  kg is the building model base mass (component c in Figure 3),  $m_b=0.1$  kg is the  
 199 mass of the aluminium part of the building model (component b) and  $m_a=0.95$  kg is the steel end mass  
 200 (component a). The latter part was added to the top of the model in order to increase the mass of the building  
 201 model so that prototype-model similitude is maintained. The mass of component d is negligible.



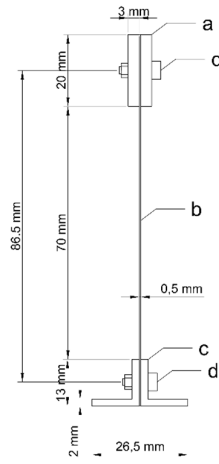


**Figure 3** Cross-section of plane building model B1 (main building)

The building model under fixed base conditions can be considered as a vertical cantilever beam of height  $h=h_B=86.5$  mm. The building model has a mass  $m_b$ , an end mass  $m_a$  and flexural rigidity  $E_m I_m=0.72$  Nmm<sup>2</sup>. Based on the formula reported in [43], the theoretical fixed base natural frequency of the building modelled as a continuous cantilever beam is

$$\omega_1 = \sqrt{\frac{k_1}{m_1}} = \sqrt{\frac{3E_m I_m}{(m_a + \frac{33}{144} m_b) h_m^3}} = 57.8 \text{ rad/s} \quad (5)$$

Also based on the study in [17] a frequency parameter is proposed for the foam-foundation as

$$\omega_2 = \sqrt{\frac{k_2}{m_2 r^2}} = \sqrt{\frac{k_f}{(m_f + m_c) r^2}} = 688.17 \text{ rad/s} \quad (6)$$

where  $k_f=10.38 \times 10^3$  N.mm/rad is the rotational stiffness and is taken as the slope of the initial tangent of the moment-rotation curve, Figure 4(b), from a lateral load test shown in Figure 4 (a). The load test was performed on the foam prior to the main testing programme on the shaking table. Two square (80 mm x 80 mm) Perspex plates representing adjacent foundations were glued firmly on the foam block. While an incremental moment is applied at one foundation plate, rotations at the centre of both plates were calculated from the vertical displacement measured. The term  $(m_f+m_c)r^2$  represents the mass rotational moment of inertia where  $r=b_m/3$  is the radius of gyration [42]. Hence the non-dimensional frequency ratio of the model is

$$\Omega = \frac{\omega_2}{\omega_1} = 11.93 \quad (7)$$

Comparing values of the mass and frequency ratios resulting from Equations (1) and (3) to those from Equations (4) and (7), yield a similitude (Prototype:Model) as follows: for mass ratio (1:0.94) and (1:0.91) for frequency ratio, in addition to the aspect ratio (1:0.94). Hence, the analogy between the prototype and the small scale model is judged to be acceptable. Despite the very good similitude achieved in the three main non-

dimensional parameters for the prototype and the model, there are other dynamic parameters of the real system not capture by the idealisation in the Appendix. The shear wave velocity of the foam is significantly lower than that in the prototype. Therefore the probagation speed of body and surface waves is likely to differ in model and prototype. This causes different arrival times of waves between prototype and model which is noticable at large spacings between the structures. However, at large spacing the SSSI is very small and so the effect of this lack of similitude is neglected. Table 1 presents a summary of the model-prototype similitude.

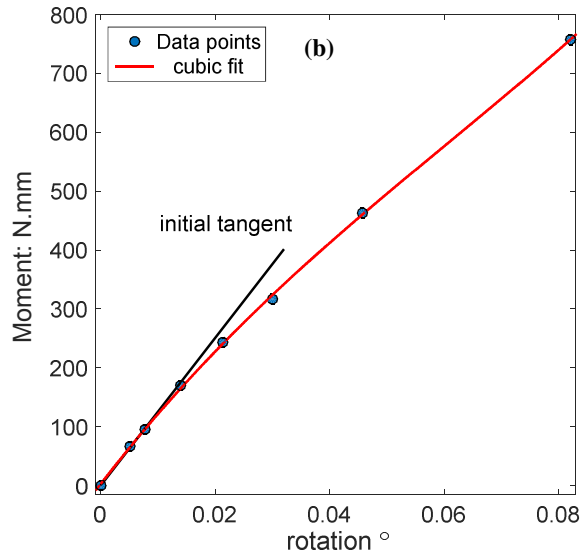
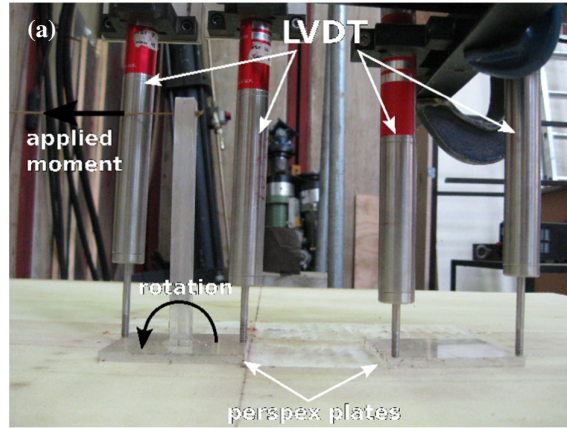


**Figure 4** (a) Load test. (b) Moment-Rotation curve of loaded foundation plate on foam.

**Table 1** Comparison of values of system parameters for prototype structure and scaled model B1.

	Units	Model	Prototype	Similitude (Prototype:Model)
Mass ratio $\alpha$	[ ]	0.266	0.25	1:0.94
Frequency ratio $\Omega$	[ ]	11.93	10.8	1:0.91
Aspect ratio $\eta$	[ ]	1.03	1	1:0.94
Aspect ratio $S_B$	[ ]	3.2	3	1:0.94
Structure's flexible-base to fixed-base frequency ratio $\Omega_f$	[ ]	0.59	0.77	1:0.76
Length	[m]	0.103	9.6	1:100
Period (fixed base)	[s]	0.1	0.303	1:3
Shear wave velocity $V_s$	[m/s]	32.3	150	1:4.76
Poisson's ratio $\mu$	[ ]	0.15	0.3	1:2
Density $\rho$	[kg/m <sup>3</sup> ]	50	1300	1:26.3

### 2.3.1 Dynamic Properties of the main model building (B1) and adjacent buildings

Free vibration tests on the main building model B1 were performed under fixed base conditions and in flexible (on foam) base condition. Fixed and flexible B1 frequencies are shown in Figure 5. Building model B1 has a fixed base natural frequency of 9.03 Hz, which agrees with the value predicted from Equation (6) with a damping ratio of 1.5 %. When attached to the foam block, the equivalent single degree of freedom natural frequency is shortened to 5.25 Hz with an increase in equivalent viscous damping ratio to 3.9 %. Simulation of this free vibration test using a 2D Finite Element (PLAXIS2D) [44] model showed similar results as shown in Figure 5.

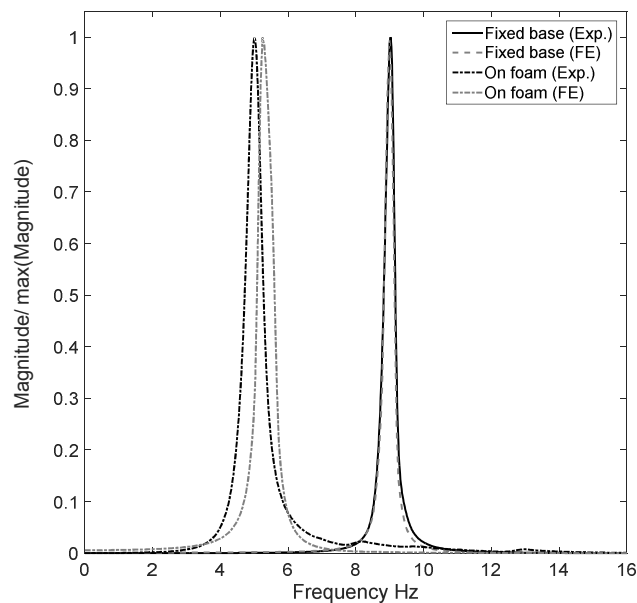


**Figure 5** Natural frequency of building B1 in fixed base and on foam conditions. Amplitude axis is normalised by maximum amplitude value.

Models of adjacent buildings used in the experiment (referred to as B2, B3, B4, B5, B6 and B7) were constructed following the same approach to that used to construct B1. Each building model has the same base dimensions and end mass; the only difference is in the height of each model. A height ratio  $\epsilon_x$  is introduced to

express the difference in height of the adjacent building models with respect to B1. So the components a and c, shown in Figure 3, are the same for all buildings models while component b is different per particular building model. It should be noted that as the central building B1 in the case of three adjacent buildings is flanked by two building models that are equal in height,  $\epsilon_x$  refers to the height ratio in both two and three adjacent buildings cases. Table 2 summarises the characteristics of adjacent building models.

**Table 2** Properties of adjacent building models

	Period (fixed base) units: s	Height ratio $\epsilon_x$	Mass ratio $\alpha$	Frequency ratio $\Omega$
B2	0.028	0.5	0.28	4.4
B3	0.063	0.75	0.27	6.3
B4	0.09	0.9	0.269	9.4
B5	0.128	1.1	0.263	19.8
B6	0.222	1.5	0.25	34.2
B7	0.357	2	0.23	55.2

Figure 6 presents the variation of mass and frequency ratios of the adjacent building model as a function of the height of building model B1. As the height of the building model adjacent to B1 increases, its mass increases which yields a lower mass ratio, hence, less soil mass contribution. On the other hand, as the height of building models adjacent to B1 decreases, its frequency increases which in turn decreases the frequency ratio and vice-versa.

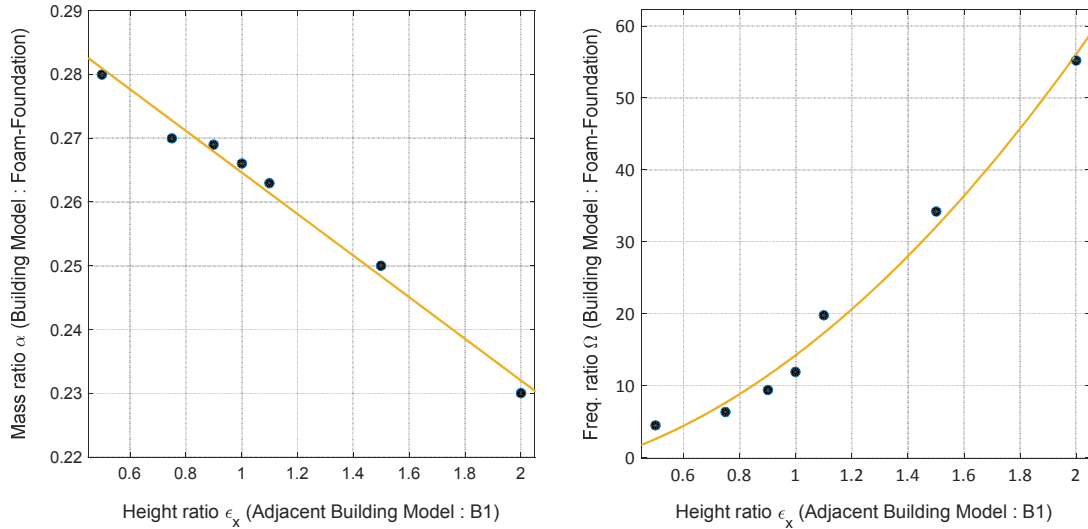


**Figure 6** Variation of experimental models mass ratio and frequency ratio with height ratio

## 2.4 Shaking Table

The large shaking table [45] at EQUALS at the University of Bristol (UK) has 6 degrees of freedom and consists of a 3 m by 3 m cast-aluminium platform capable of carrying a maximum load of 15 tonnes with an operating frequency range of 0-100 Hz and its platform has a first flexural natural frequency of 100 Hz. The shaking table is operated via a digital controller which is controlled by a Personal Computer (PC). The PC provides motion control that allows the application of a wide range of real earthquakes, sinusoidal and random

signal forms. Data can be collected on up to 64 channels on a separate data acquisition computer system that is synchronised to the main control computer.

## 2.5 Instrumentation and data acquisition

Ten 3-axis ADXL335 Micro Electro Mechanical Systems (MEMS) [46] based accelerometers of 18x18x1.6 mm<sup>3</sup> size were used to measure acceleration responses. The MEMS accelerometers measure acceleration with a minimum full-scale range of  $\pm 3$  g. They can measure the static acceleration of gravity in tilt-sensing applications, as well as dynamic acceleration resulting from motion, shock, or vibration. The accelerometers were calibrated against a standard piezoelectric accelerometer (manufactured by SETRA) having a calibration factor of 1 volt/g used at the EERC laboratory. Four accelerometers were attached at the foam's surface using a strong epoxy adhesive, one at the middle edge and another at one corner, with the remaining two placed between building models, as illustrated in Figure 7(a). Building models were each instrumented with two accelerometers, one at the top and one at the base, as shown in Figure 7(b). In addition, three single axis piezoelectric accelerometers were also attached to the shaking table platform in each direction (x, y and z). Figure 8 (a), (b), (c) and (d) show examples for different cases of buildings on foam and for the experimental system on the shaking table.

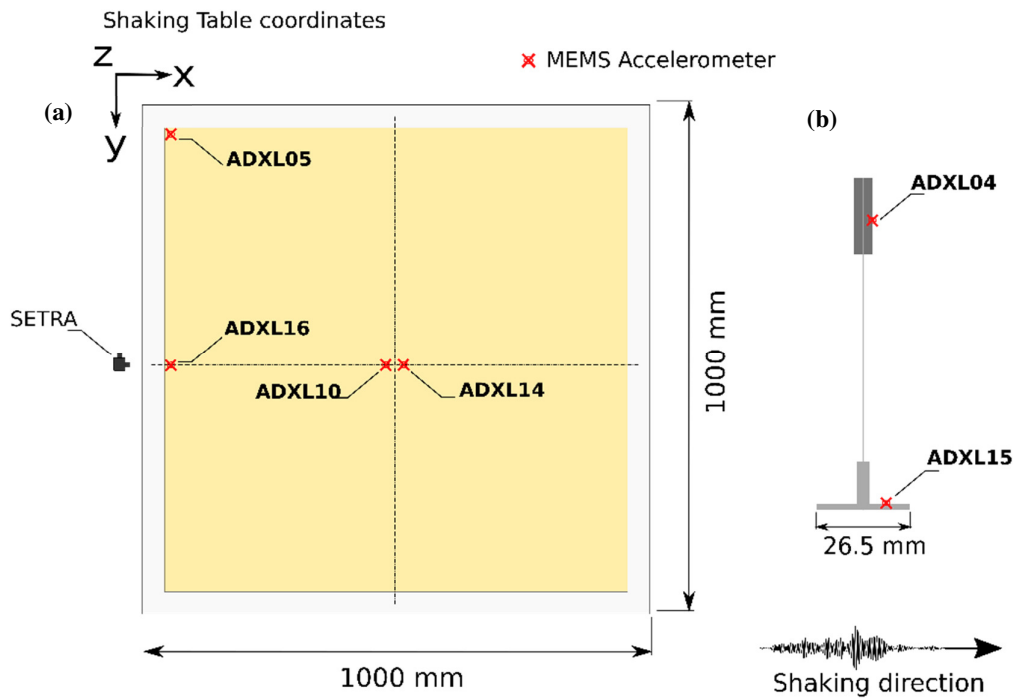


**Figure 7** Transducer positions: (a) accelerometers on foam; (b) accelerometers on building. (Not to scale)

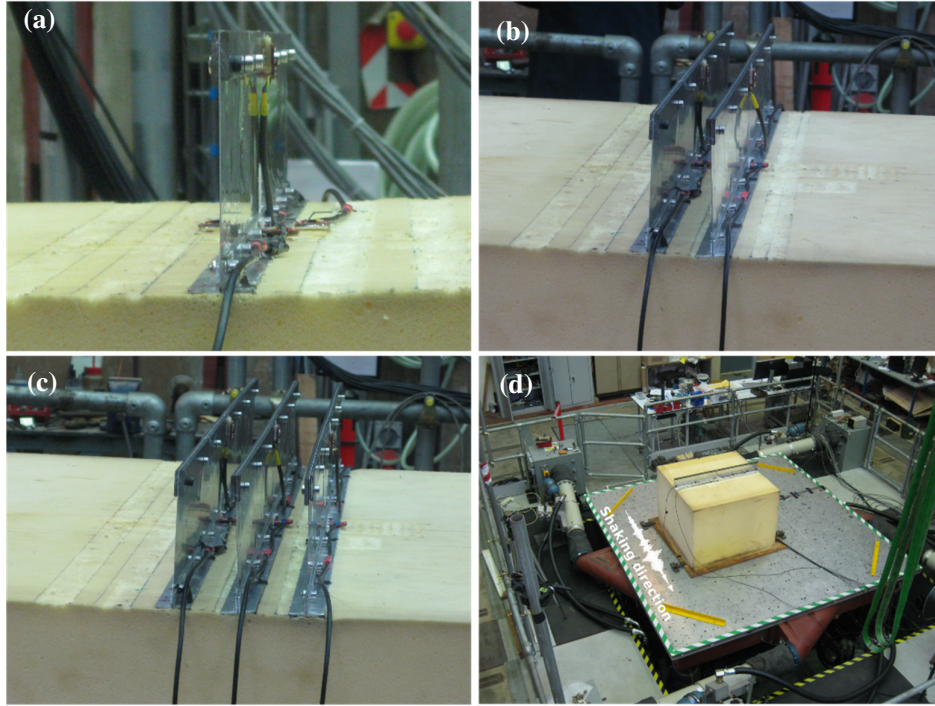


**Figure 8** Overview of experiment: (a) single building; (b) two identical buildings; (c) three identical buildings; (d) experimental system mounted on the shaking table.

After setting up and instrumenting the foam and building models, the foam was firmly clamped to the shaking table platform. Each accelerometer was connected to an amplifier to improve the signal to noise ratio. The amplifier in turn was connected to a low pass 80 Hz digital filter, then to the individual channels of the data acquisition system located in the EERC control room. A total of up to 30 channels of the data acquisition system were dedicated to any experiment. The acquired accelerometer data was subsequently post-processed using MATLAB [47].

### 3 Experimental Program

A single building case, *uncoupled* SSI system, was tested first, then its behaviour was used as a benchmark for further tests with adjacent buildings added to the system at a specified separation distance  $Z$ , at which point it became a *coupled* SSSI system. Broadly, there are two cases of adjacency herein, a case when B1 is flanked by one building model and another case when it is flanked by two building models, one on either side. In all cases, the adjacent buildings were separated at a distance equal to the width of building model  $Z=b_m$ . The uncoupled and coupled systems were subjected to two types of excitations: (i) white noise for system identification; and (ii) a set of five earthquake records. 15 different configurations were tested under various conditions of adjacency categorised by the height ratio  $\epsilon_x$  as tabulated in Table 3 and depicted in Figure 9. Each of these configurations was tested under the two types of excitations for a total of 90 individual tests.

305

**Table 3** Test configurations

PART I			PART II		
SINGLE BUILDING					
[B1-I]			[B1-II]		
TWO ADJACENT BUILDINGS					
			[2B-1]	$\varepsilon_x=0.5$	$Z=b_m$
			[2B-2]	$\varepsilon_x=0.75$	$Z=b_m$
[2B-3]	$\varepsilon_x=0.9$	$Z=b_m$			
[2B-4]	$\varepsilon_x=1$	$Z=b_m$			
[2B-5]	$\varepsilon_x=1.1$	$Z=b_m$			
			[2B-6]	$\varepsilon_x=1.5$	$Z=b_m$
			[2B-7]	$\varepsilon_x=2$	$Z=b_m$
THREE ADJACENT BUILDINGS					
			[3B-1]	$\varepsilon_x=0.5$	$Z=b_m$
			[3B-2]	$\varepsilon_x=0.75$	$Z=b_m$
[3B-3]	$\varepsilon_x=0.9$	$Z=b_m$			
[3B-4]	$\varepsilon_x=1$	$Z=b_m$			
[3B-5]	$\varepsilon_x=1.1$	$Z=b_m$			
			[3B-6]	$\varepsilon_x=1.5$	$Z=b_m$
			[3B-7]	$\varepsilon_x=2$	$Z=b_m$

306

307

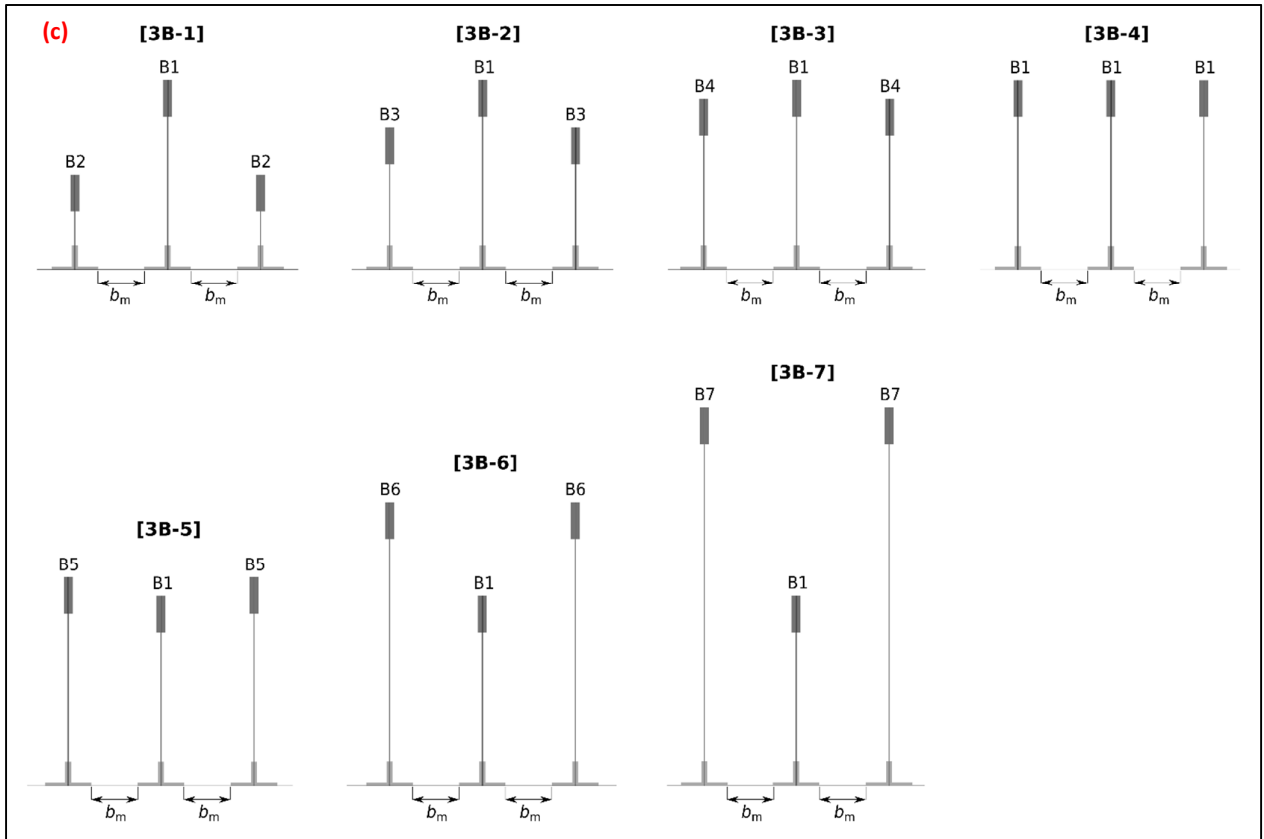
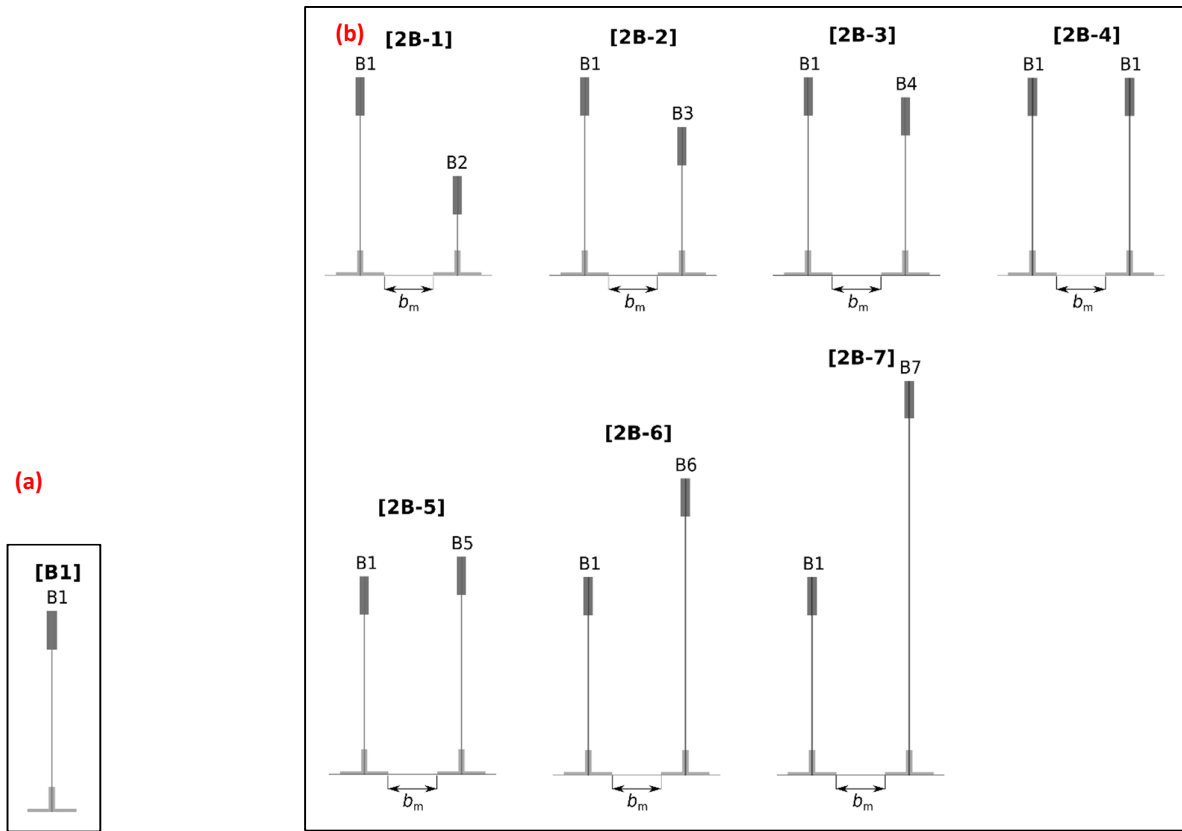


**Figure 9** Building models configurations, (a) single building, (b) two adjacent buildings, (c) three adjacent building.



Due to the very busy schedule of the shaking table facility, the experimental program was conducted in two parts (Part I and Part II) separated by about one month in time. As preliminary analytical results from the study in [17] has suggested that the most extensive interaction effect would occur when adjacent buildings are of similar but not identical heights, in the first part of testing three height ratio variations were considered ( $\epsilon_x=0.9, 1, 1.1$ ). The remaining of height ratios were considered in the second part. Hence, the benchmark single building model B1 was tested twice at the beginning of each experimental part and therefore denoted by [B1-I] and [B1-II]. The difference between these two particular single buildings cases is that in the first case it was only the B1 model placed on the foam surface while in the latter test a number of building model bases (only component c, refer to Figure 3) were already present on the foam. The presence of these bases was inevitable due to the fact that they were already permanently attached to the foam from the previous testing in Part-I and their removal would have damaged the foam surface.

### 3.1 Input Excitation

The experimental SSSI system was subjected to two types of excitations, namely, a random white noise (with an RMS amplitude of  $\approx 0.1g$ ) and a set of uniaxial horizontal components of five earthquake events, as summarised in Table 4. The earthquake records were obtained from the PEER ground motion database [48]. All ground motions were recorded on weak soils, which correspond to sites of an average shear wave velocity of less than 180 m/s. These records were scaled down in amplitude and duration in accordance to the similitude factors in Table 1. The time-scaling factor is  $SF_T=T_M/T_P\approx 0.33$ , where  $T_M$  and  $T_P$  are the fixed base periods of the building model and prototype respectively. The length-scaling factor is  $SF_L=L_M/L_P\approx 0.01$ , where  $L_M$  and  $L_P$  are the total heights of building model and prototype respectively. So for accelerations to be scaled in amplitude, they should be multiplied by  $SF_T/SF_L^2=0.09$  (i.e. dimensionless Length/Time<sup>2</sup>). Figure 10 shows the original unscaled and scaled signals. The number of data points of scaled signals was kept the same as the original PEER signals ( $dt = 0.005s$  i.e. a sampling frequency of 200 Hz). The elastic response spectra for nominal 5% damping of the amplitude and time scaled earthquake ground motions show that all building model natural periods lie within the region of interest (Figure 11).

**Table 4** Earthquake records, retrieved from Pacific Earthquake Engineering Research Center (PEER) Database (2000) [48] and their scaled magnitudes.

Earthquake Event	Duration s	Closest Distance to Rupture Plane (km)	Scaled Duration s	Peak Ground Acceleration PGA m/s <sup>2</sup>	Scaled PGA m/s <sup>2</sup>
Morgan Hill P0459 04/24/84	35.99	9.87	11.99	0.45	0.041
Loma Prieta P0790 10/18/89	39.95	87.87	13.32	0.98	0.089
Imperial Valley P0175 10/15/79	39.54	17.94	13.18	2.612	0.23
Duzce P1536 11/12/99	86.16	188.7	28.37	0.376	0.034
Westmorland P0320 04/26/81	28.74	19.37	9.58	1.952	0.175

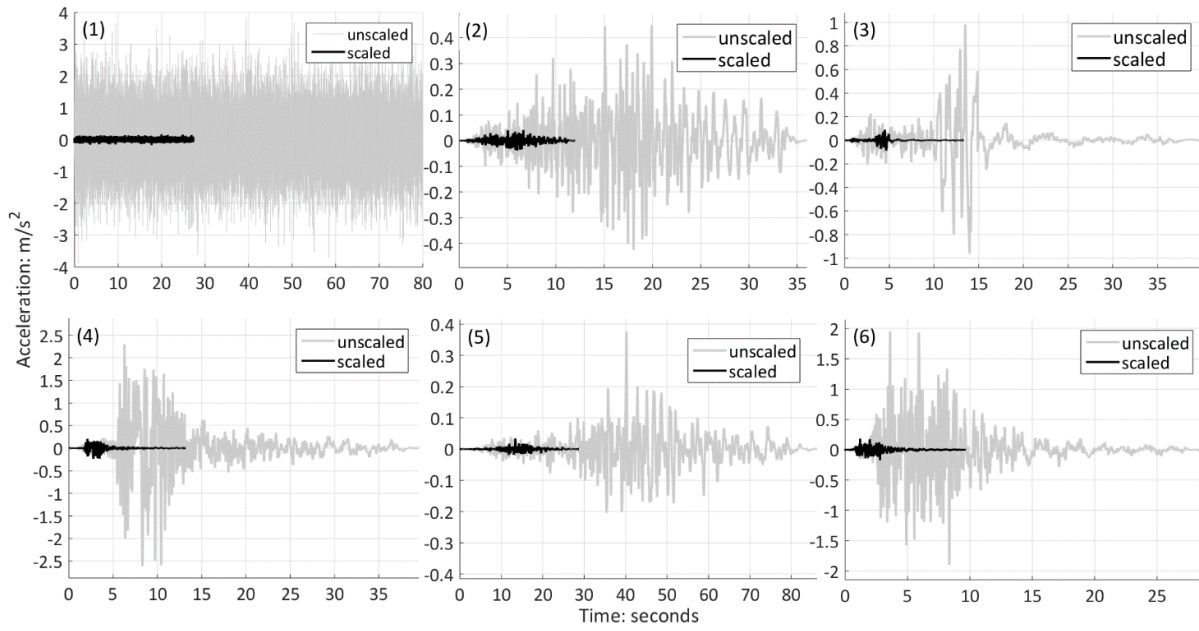


**Figure 10** Un-scaled and scaled earthquake signals, (1) white noise, (2) Morgan Hill, (3) Loma Prieta, (4) Imperial Valley, (5) Duzce and (6) Westmorland.

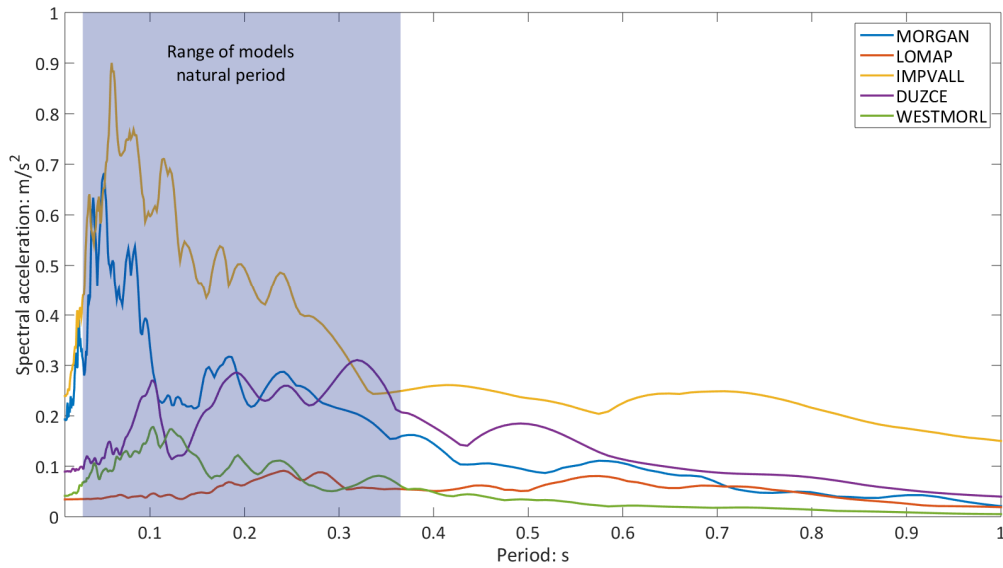


**Figure 11** Elastic response spectra of scaled earthquake records.

## 4 Results

As has been stated earlier, the single building model case (uncoupled SSI case) was tested twice, in [B1-I] and [B1-II]. In order to conduct consistent assessments i.e. uncoupled (SSI) vs. coupled (SSSI); comparisons of spectral power were made with respect to the relevant uncoupled case in each part. Figure 12 compares the transfer functions (base to top of building model B1) which resulted from subjecting it to the white noise excitation for both cases. There is a slight increase in the response power (10.6%) and natural frequency (3.7%) of B1 in Part-II, which might be attributed to the stiffening effect imposed on the foam by the presence of building model bases along its surface.

As a primary system performance measure, the change in total acceleration power (spectral power) of building model B1 caused by its interaction with adjacent building models has been calculated. Transfer function  $TF(\omega)$  estimates have been calculated for all interaction cases considered.  $TF(\omega)$  is defined as the quotient of the power spectral density (PSD) of an output signal and the power spectral density of an input signal. In this study, the input signal is taken as the acceleration response recorded at base level of B1 while the output signal is taken as the acceleration response at the top of B1.

The percentage change in total acceleration power denoted by  $\chi'_{B1}$  between uncoupled and coupled cases of building model B1 is calculated as the difference in the area under each transfer function curve as

$$\chi'_{B1} = 100 \cdot \frac{\int_{-\infty}^{\infty} TF(\omega) d\omega_{(coupled)} - \int_{-\infty}^{\infty} TF(\omega) d\omega_{(uncoupled)}}{\int_{-\infty}^{\infty} TF(\omega) d\omega_{(uncoupled)}} \quad (8)$$

The total power of a time-series, which is based on all data points, is a more robust statistical estimator of performance than the signal peak which is based on one point [49]. Additionally, the use of transfer function as a means of assessing the change in power of the response of B1 due to its interaction with other buildings is advantageous in the sense that any possible effect of the foam in amplifying the response of B1 would be excluded, i.e. site amplification.

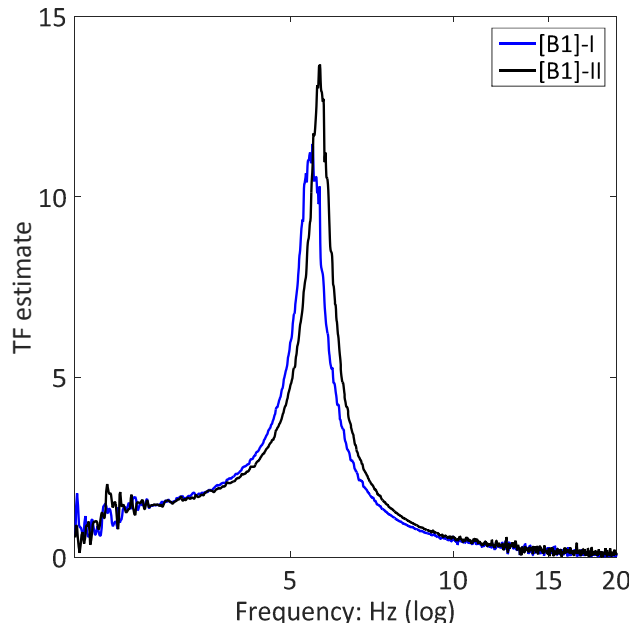


**Figure 12** Transfer functions of single building mode B1 during testing parts [B1-I] and [B1-II].

#### 4.1 Response under White Noise Excitation

For the two adjacent buildings case, Figure 13 (a) and (b) show transfer functions for the uncoupled B1 building in comparison to the coupled B1 case for the particular configurations obtained experimentally in part I and part II. Figure 14 (a) and (b) show similar plots for the case of three adjacent buildings. As suggested in former

analytical studies [17, 18] the worst interaction effect occurs when a building is adjacent to similar (not less than 10% difference in height) but not identical buildings. In the case when B1 is adjoined by slightly taller building model(s) B5, i.e.  $\varepsilon_x=1.1$ , it suffers the highest amplification in spectral power. This amplification is approximately 16% and 21% respectively when one and two adjacent B5 buildings are present. On the other hand, the presence of one or two adjacent shorter building models B3 at  $\varepsilon_x=0.75$  respectively causes the highest attenuation of B1's spectral power by approximately 6% and 16%. When adjacent buildings are identical,  $\varepsilon_x=1$ , there is an increase in spectral power of up to 10%. Very small effects of interaction,  $< 5\%$ , are observed for greater and lower height ratios (i.e.  $\varepsilon_x \geq 1.5$  and  $\varepsilon_x \leq 0.5$ ). It is also noted that there is a slight increase in the estimated natural frequency of B1 compared to that measured from free vibration tests but the damping ratio remains as previously measured at around 3.9%.

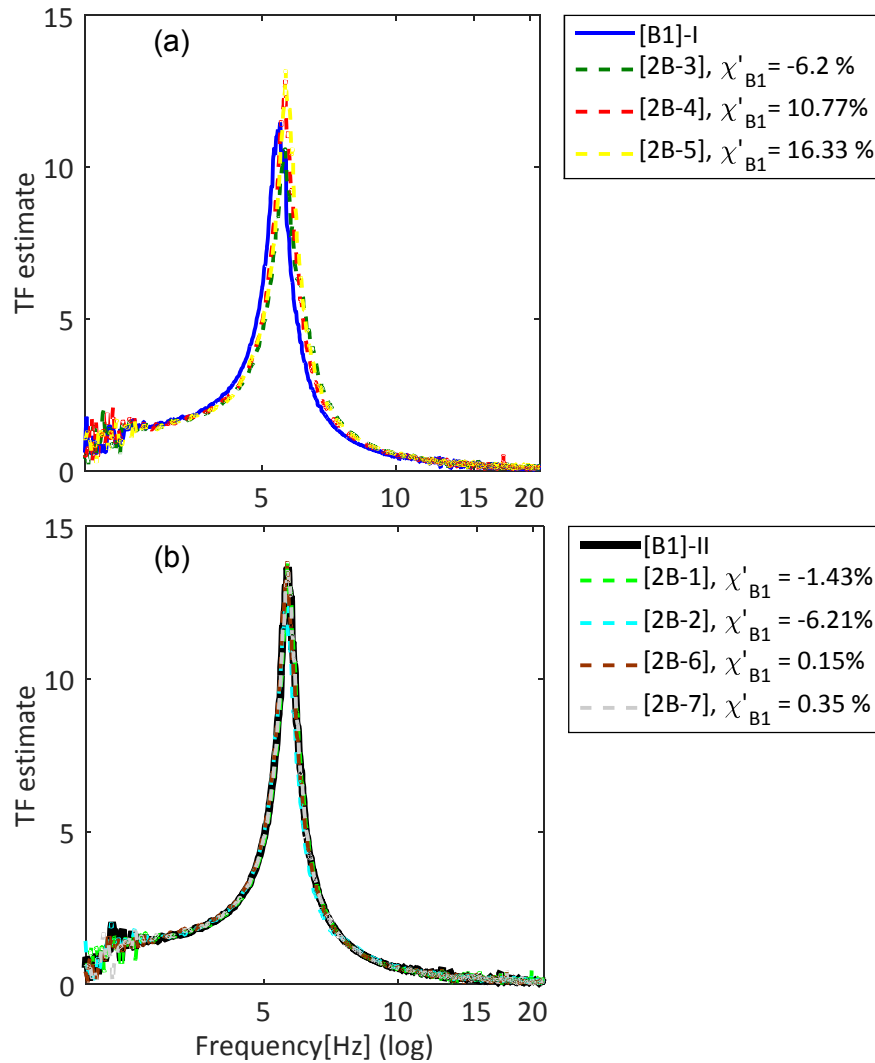


**Figure 13** Uncoupled and coupled frequency of B1- case of two adjacent buildings (a) Part I, (b) Part II.

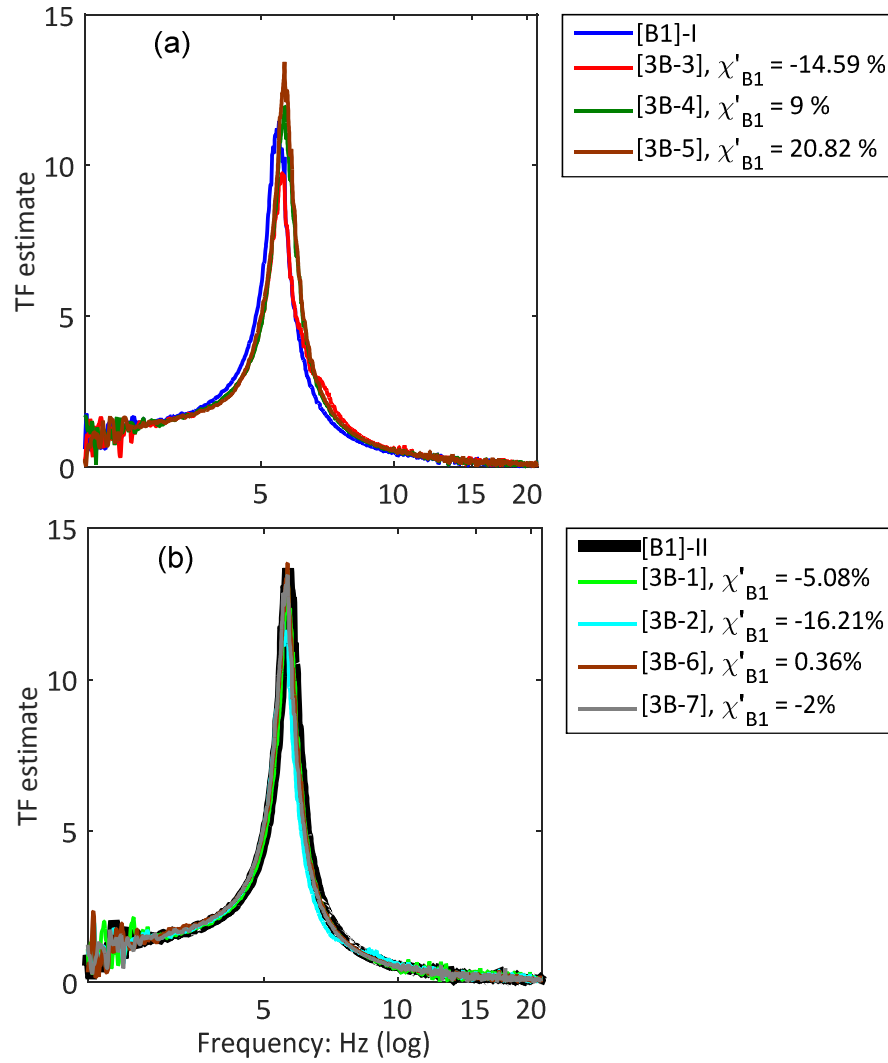


**Figure 14** Uncoupled and coupled frequency of B1- case of three adjacent buildings (a) Part I, (b) Part II.

The aforementioned effects of variation in adjacent buildings heights on B1 spectral power could collectively be seen in the S shape curves shown in Figure 15. The dashed horizontal line at zero % represents the case of no interaction effect and values of  $\chi'_{B1}$  above the dashed line represent a detrimental SSSI effect (increase of spectral power) while the beneficial values (decrease of spectral power) are below the dashed line. Clearly, the presence of two buildings has a greater interaction impact than the presence of only one building. In addition, the experimental data points compare well with the lines from analytical studies using low order discrete models for the case of two [17] and three [18] adjacent buildings.

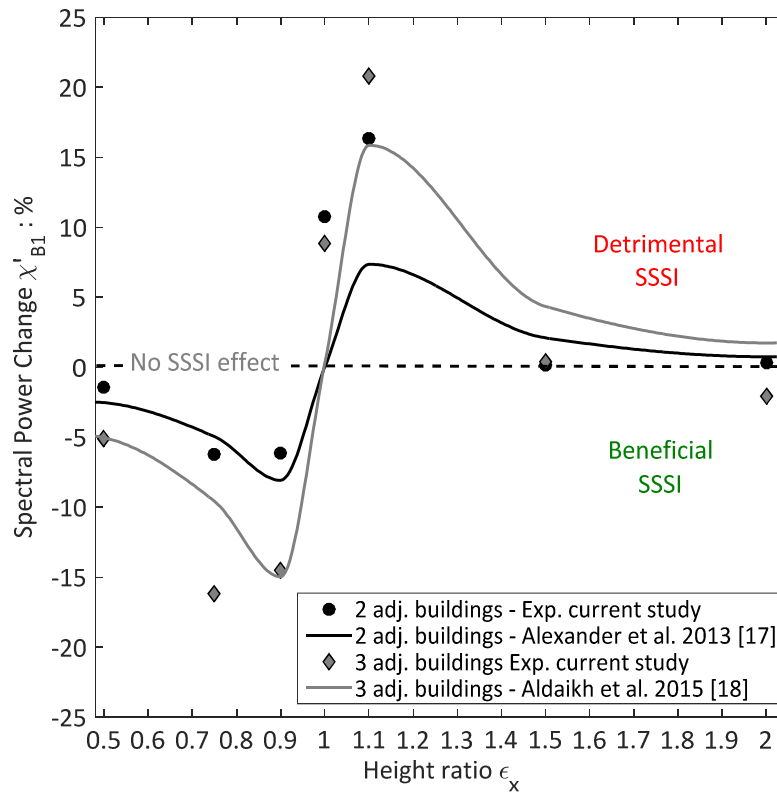


**Figure 15** Change of B1 spectral power with the variation in height of adjacent buildings subjected to white noise and comparison to analytical results.

## 4.2 Response under Earthquake Excitation

For the selected range of earthquake records, power spectra were evaluated for different configurations of two and three building cases and compared to that of a single building case B1. For every configuration the mean of the percentage change in spectral power (denoted by  $\chi_{B1}$  to be distinguished from  $\chi'_{B1}$  of the white noise excitation) resulting from the five earthquake records was calculated.

Figure 16 shows the variation in the percentage change in spectral power against the change in height ratio for the case of two adjacent buildings and three adjacent buildings. The *S* shape of the curves shown in this figure are comparable to those shown in Figure 15 for the case of white noise excitation, though in the case of earthquake motions the magnitude of the change in power is larger. Each of the data points shown represents an average across the 5 earthquake motions. The range of maximum and minimum values of  $\chi_{B1}$  measured for each height ratio is also depicted. For the case of two buildings, a maximum amplification up to 56% at a height ratio  $\epsilon_x=1.1$  and a maximum attenuation up to 18% at  $\epsilon_x=0.75$  could be observed. Similarly at the height ratio  $\epsilon_x=1.1$  for the case of three buildings a maximum amplification up to 40% and a maximum attenuation up to 31% at  $\epsilon_x=0.75$  are observed. No significant change in the spectral power of B1 was observed at height ratios greater than 1.1.

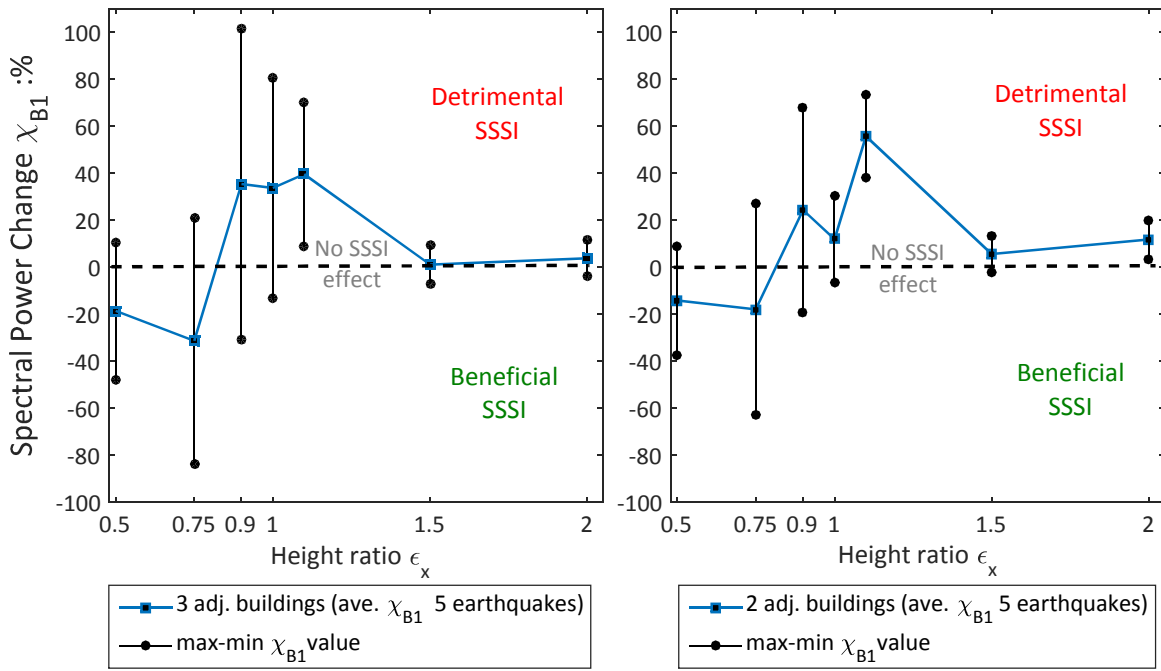


**Figure 16** Change of B1 average spectral power with the variation in height of adjacent buildings subjected to several earthquake motions.

Another system performance measure is introduced to complement the earlier stated observations and provide a comparison with results from a previous experimental study conducted using centrifuge testing of two adjacent structures having shallow foundations resting on sand [30]. Figure 17 shows the peak acceleration response of building model B1 averaged across the 5 motions in various two adjacent buildings cases normalised by that of single B1 case. So here the dashed horizontal line at 100% is the “no SSSI effect” line. The horizontal axis represents the fixed base period ratio, that is the period of adjacent building models (B1 to B7) to the period of building model B1. Peak acceleration may be expected to correlate more directly to the peak demand force that the structural elements must resist, in contrast to spectral power which may be a better indicator of total energy input and therefore cumulative damage.

Again the interaction effect across different buildings appears to be governed by the S shape curve, despite representing a different interaction effect measure. It can be seen that the most significant detrimental interaction effect occurs at a period ratio of approximately 1.17 which corresponds to a height ratio  $\epsilon_x=1.1$ . In this case the peak acceleration response of B1 increases by about 26%. Conversely, the most beneficial effect occurred at period ratio of 0.58 which is the case when  $\epsilon_x=0.75$  where the peak acceleration response decreased by approximately 25 %.

In Knappett et al.[30], two cases of similar (period ratio of 1) and dissimilar (period ratio of 1.475) model buildings were tested in the centrifuge under the Kobe 1995 ground motion. The ground motion was rescaled and applied in a series of shocks; a 0.1g small pre-shock; a 0.5g main shock and a final 0.1g motion to provide a recharacterisation of the behaviour at smaller strains following the substantial changes imparted to the soil fabric by the preceding motions. Data for the smaller of the two structures was used, having a prototype fixed

base natural period of 0.33 s, as this was closest to the natural period of B1 in the shaking table tests (0.303 s). Although the results for the case of similar buildings shows a similarity with the result from current study, there is a noticeable difference in the case of dissimilar buildings.

This difference is understandable as the centrifuge study was conducted using real granular soil which is highly non-linear and inelastic while the current study is limited to purely linear elastic behaviour. The non-linearity within the centrifuge tests appeared to attenuate the detrimental SSSI effect on peak acceleration response. This suggests that analytical solutions based on a linear elastic subgrade idealisation (e.g.[17]) may provide conservative estimates of SSSI effects, though this requires further verification through further experimental and numerical studies.

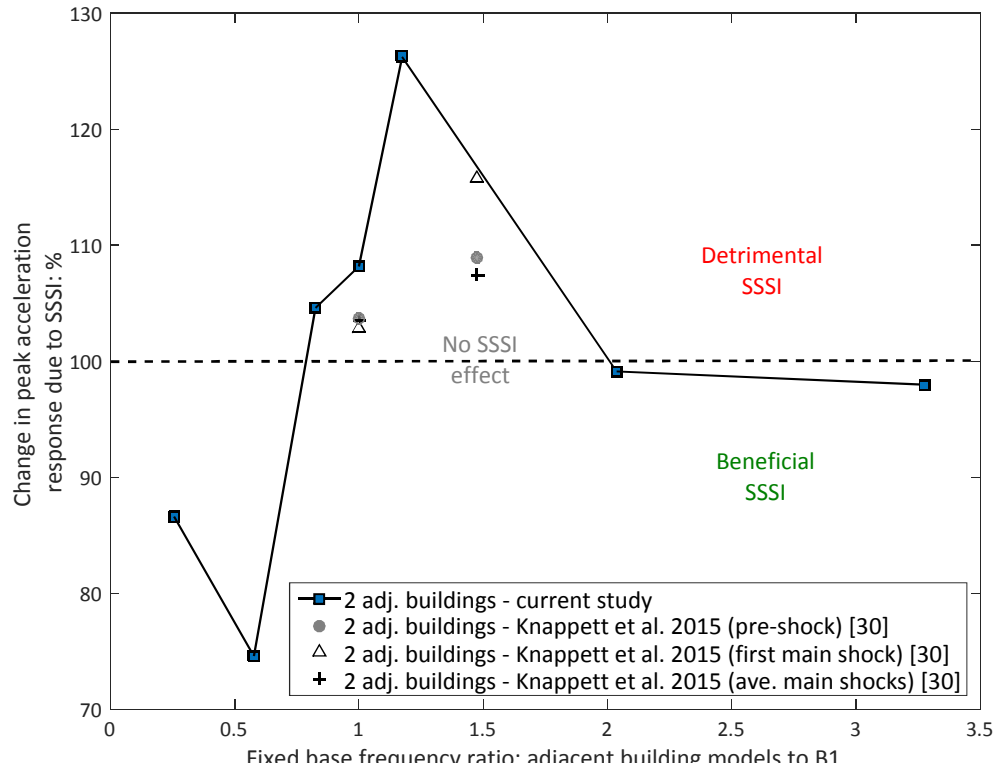


**Figure 17** Effect of SSSI on the peak acceleration of B1 and comparison to a centrifuge study in [30].

## 5 Comparison to Finite Element simulation

In order to have further confidence in the experimental measurements and their reliability, a series of analogous plane strain Finite Element models were created using PLAXIS2D to numerically replicate some of the experimental configurations. Three cases were considered: (i) single B1 (config. [1B]-I), (ii) two adjacent identical B1 models (config. [2B-4]) and (iii) three adjacent identical B1 models (config [3B-4]) under white noise excitation (duration = 80 seconds). The excitation applied at the bottom of the finite element mesh was the horizontal acceleration component in the direction of shaking recorded at the shaking table platform level. An example of the finite element model is depicted in Figure 18 for the case of a single building and models for the rest of the cases considered were created in a similar manner.



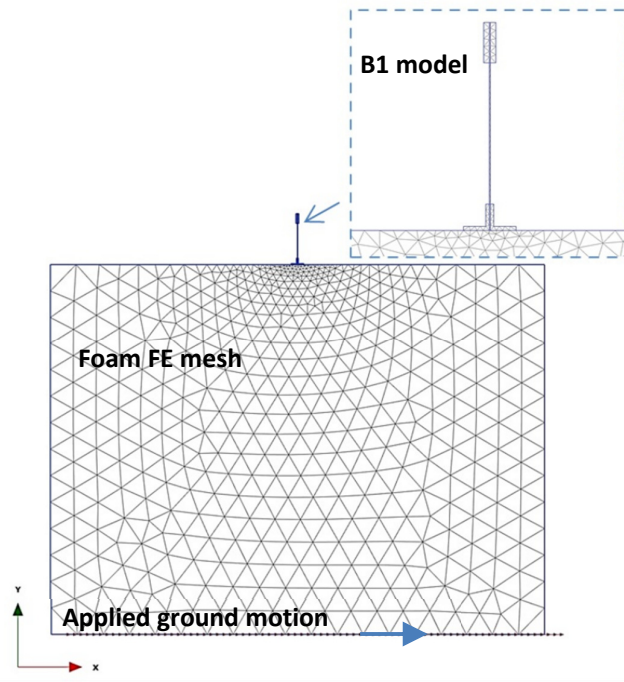


**Figure 18** An example of 2D Finite Element mesh of the experimental model for the case [1B]-I.

Figure 19 and Figure 20 respectively show normalised (with respect to the uncoupled single B1 case) frequency responses of the uncoupled B1 building in comparison to the coupled B1 model for the case of two and three adjacent buildings. The figures also compare results obtained experimentally and numerically. Observations from the two figures show a very good agreement, with the average percentage difference between the experimental and numerical models being less than 7% in terms of frequency estimation and less than 28% in terms of change in spectral power estimation.

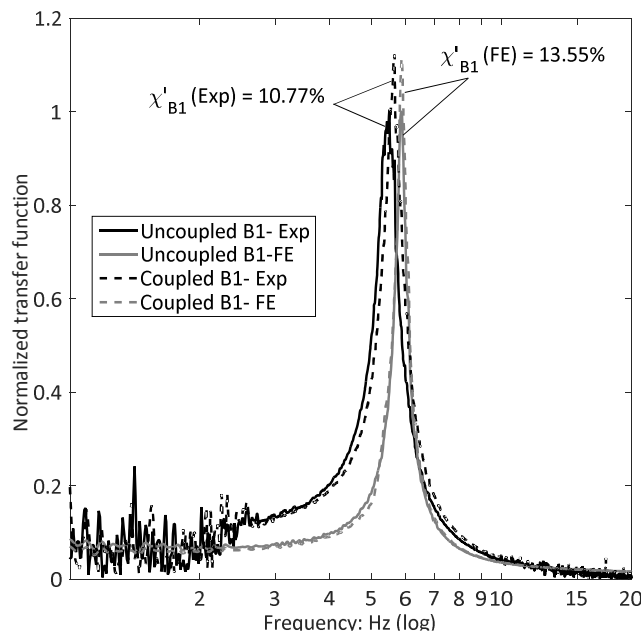


**Figure 19** Experimental and numerical uncoupled and coupled responses of building model B1, two identical adjacent buildings case.

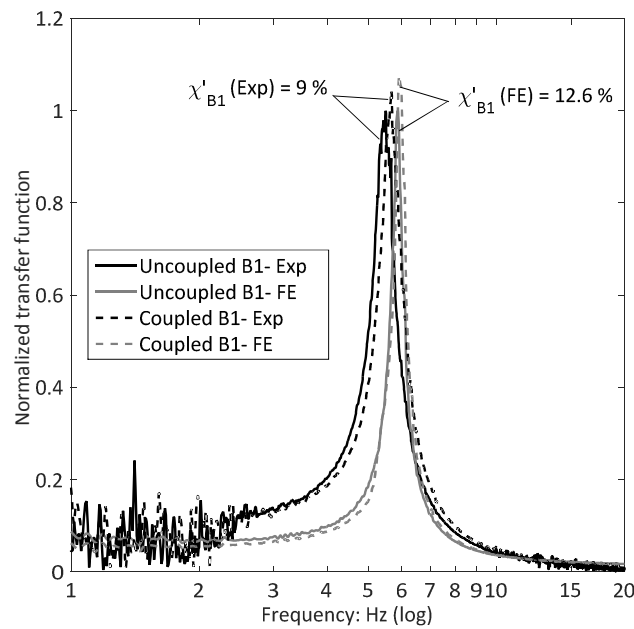


**Figure 20** Experimental and numerical uncoupled and coupled responses of building model B1, three identical adjacent buildings case.

## 6 Conclusion

This paper reported a small-scale parametric shaking table experimental investigation to study the problem of Structure-Soil-Structure interaction. Buildings were modelled using plates made of aluminium with steel end strips mounted on an elastic soil substitute material. Different parametric configurations of groups of two and three adjacent buildings were tested under the excitation of white noise and earthquake ground motions.

As indicated by previous low order analytical modelling [17, 18] by the authors, the current work showed that the interaction effect could be beneficial or detrimental on the structural response depending on the geometrical characteristics of the adjacent buildings, specifically their height. The experiments conducted herein have also validated those low order models and their applicability for the cases of two and three adjacent buildings. Interestingly, for the adjacency cases considered in this study, it appears that there is a predominant *S* shape function governing the relationship between the interaction effect and the variation of height of adjacent buildings. This alternate relationship existed regardless of the number of buildings (2 or 3 adjacent buildings) or the system performance measure used.

A building appears to undergo the most detrimental interaction effect when flanked by either one or two longer period buildings which are 10% greater in height or 20% different in fixed base natural period. This effect is apparent in both the spectral power and peak acceleration response of the structure as a result of its interaction via the mutual ground connecting it with adjacent buildings. On the other hand, the highest reduction or beneficial effect is observed when the building is flanked by neighbouring structures with shorter periods or 10-25% shorter in height. In comparison to another experimental SSSI study on centrifuge, results showed that spectral power change could be utilised as a very good indication to the beneficial and detrimental SSSI effects

in terms of the change in acceleration response which would correspondingly affect the demands on base shear and overturning moments acting on the structure. Changes of up to  $\pm 25\%$  in peak acceleration could result from the adjacent buildings' mutual interaction. Finite Element replica models of selected experimental configurations provided confidence in the results presented.

Undoubtedly there are a considerable number of structural and soil parameters involved in the study of such a complex interaction problem; this experimental work tried to simplify the problem while maintaining the important features of the problem without oversimplification. Results of the current study could serve as a first order estimate for the seismic power, i.e. risk, which could be transferred to and from a certain structure as a result of its interaction with up to two neighbouring structures under dynamic excitation.

#### **Acknowledgement**

The researchers are very grateful for the support of the Faculty of Engineering, staff and technicians of the Earthquake Engineering Research Centre at the University of Bristol. The Ministry of Higher Education and Omar Al-Mukhtar University, Albayda, Libya have granted financial support during this research.

## 503    **References**

- 504    [1] V.V. Bertero, Connections The EERI Oral History Series, Earthquake Engineering Research Institute,  
505    2009.
- 506    [2] L. Menglin, W. Huaifeng, C. Xi, Y. Zhai, Structure–soil–structure interaction: Literature review, Soil  
507    Dynamics and Earthquake Engineering, 31 (2011) 1724-1731.
- 508    [3] M.M. Zaman, Influence of Interface Behavior in Dynamic Soil-Structure Interaction Problems, in, PhD  
509    Thesis, University of Arizona, 1982.
- 510    [4] J.E. Luco, L. Contesse, Dynamic structure-soil-structure interaction, Bulletin of the Seismological Society  
511    of America, 63 (1973) 1289-1303.
- 512    [5] T Kobori, R. Minai , K. Kusakab, Dynamical Characteristics of Soil-Structure Cross-Interaction System,  
513    Bulletin of the Disaster Prevention Research Institute, Kyoto University, 22 (1973).
- 514    [6] T. H. Lee, D.A. Wesley, Soil-Structure Interaction of Nuclear Reactor Structures Considering Through-  
515    Soil Coupling between Adjacent Structures, Nuclear engineering and design, 24 (1973) 374-387.
- 516    [7] H.L. Wong, M.D. Trifunac, Two-dimensional, antiplane, building-soil-building interaction for two or more  
517    buildings and for incident planet SH waves, Bulletin of the Seismological Society of America, 65 (1975) 1863-  
518    1885.
- 519    [8] J. Lysmer, H. Bolton, Seed, T. Udaka , R. N. Hwang, C.F. Tsai, Efficient Finite Element Analysis of  
520    Seismic Structure-Soil-Structure Interaction, in, Earthquake Engineering Research Center, College of  
521    Engineering, University of California, Berkeley, 1975.
- 522    [9] W. Matthees, G. Magiera, A sensitivity Study of Seismic Structure-Soil-Structure Interaction Problems for  
523    Nuclear Power Plants, Nuclear Engineering and Design, 73 (1982) 343-363.
- 524    [10] J. Qian, D.E. Beskos, Dynamic interaction between 3-D rigid surface foundations and comparison with  
525    the ATC-3 provisions, Earthquake Engineering & Structural Dynamics, 24 (1995) 419-437.
- 526    [11] L. Lehmann, H. Antes, Dynamic structure-soil-structure interaction applying the Symmetric Galerkin  
527    Boundary Element Method (SGBEM), Mechanics Research Communications, 28 (2001) 297-304.
- 528    [12] S. Wang, G. Schmid, Dynamic structure-soil-structure interaction by FEM and BEM, Computational  
529    Mechanics, 9 (1992) 347-357.
- 530    [13] L. A. Padron, J. J. Aznarez, O. Maeso, Dynamic structure–soil–structure interaction between nearby piled  
531    buildings under seismic excitation by BEM–FEM model, Soil Dynamics and Earthquake Engineering, 29  
532    (2009) 1084-1096.
- 533    [14] M. Ghandil, F. Behnamfar, M. Vafaeian, Dynamic responses of structure–soil–structure systems with an  
534    extension of the equivalent linear soil modeling, Soil Dynamics and Earthquake Engineering, 80 (2016) 149–  
535    162.
- 536    [15] N.A. Alexander, E. Ibraim, H. Aldaikh, Exploration of structure-soil-structure interaction dynamics, in:  
537    Thirteenth International Conference on Civil, Structural and Environmental Engineering Computing, Civil-  
538    Comp Press, Strelingshire, UK, Paper 216, Crete, 2011.
- 539    [16] H. Aldaikh, N.A. Alexander, E. Ibraim, Discrete Model for Dynamic Structure-Soil-Structure Interaction,  
540    in: The Fifteenth World Conference on Earthquake Engineering, Lisbon, Portugal, 2012.
- 541    [17] N. A. Alexander, E. Ibraim, H. Aldaikh, A Simple Discrete Model for Interaction of Adjacent Buildings  
542    During Earthquakes, Computers & Structures, 124 (2013) 1-10.

543 [18] H. Aldaikh, N.A. Alexander, E. Ibraim, O. Oddbjornsson, Two Dimensional Numerical and Experimental  
544 Models for the Study of Structure-Soil-Structure Interaction Involving Three Buildings, Computers and  
545 Structures, 150 (2015) 79-91.

546 [19] P. B. Mattiesen, R.B. MacCalden, Coupled response of two foundations, in: 5th World Conference on  
547 Earthquake Engineering, Rome, Italy, 1974.

548 [20] T. Kobori, R. Minai, K. Kusakabe, Dynamical Cross-Interaction Between Two Foundations, in: 6th  
549 World Conference on Earthquake Engineering, New Delhi, India, 1977, pp. 1484–1489.

550 [21] R. Shohara, I. Kurosawa, Y. Shinozaki, D. Sakamoto, Tests on Dynamic Interaction between Foundations,  
551 in: 10th World Conference on Earthquake Engineering, Balkerna, Rotterdam, 1992.

552 [22] Y. Shimomura, K. Oshima, Y. Ikeda, R. Kondo, M. Nakanishi, H. Adachi, A Fundamental Study on  
553 Dynamic Cross Interaction of Adjacent Structures Supported on Pile Foundations, in: Structural Mechanics  
554 in Reactor Technology SMiRT 16, Washington, 2001, pp. Paper #1518.

555 [23] T. Yano, Y. Kitada, M. Iguchi, T. Hirotani, K. Yoshida, Model Test on Dynamic Cross Interaction of  
556 Adjacent Building In Nuclear Power Plants Overall Evaluation on Field Test, in: 17th International  
557 Conference On Structural Mechanics in Reactor Technology., 2003.

558 [24] Y. Kitada, M. Iguchi, Model Test on Dynamic Cross Interaction of Adjacent Buildings In Nuclear Power  
559 Plants- An Outline and Outcomes of the Project, in: 13th World Conference on Earthquake Engineering,  
560 Vancouver, B.C., Canada, 2004.

561 [25] T. Yano, Y. Kitada, M. Iguchi, T. Hirotani, K. Yoshida, Model Test on Dynamic cross Interaction of  
562 Adjacent Buildings in Nuclear Power Plants, in: 12th World Conference on Earthquake Engineering, New  
563 Zealand, 2000.

564 [26] Y. Kitada, T. Hirotani, M. Iguchi, Models Test on Dynamic Structure–Structure Interaction of Nuclear  
565 Power Plant Buildings, Nuclear Engineering and Design, 192 (1999) 205-216.

566 [27] P.Z. Li, X.Y. Hou, Y.M. Liu, X.L. Lu, Shaking Table Model Tests on Dynamic Structure-Soil-Structure  
567 Interaction during Various Excitations in: 15th World Conference on Earthquake Engineering, Lisbon,  
568 Portugal, 2012.

569 [28] N.W. Trombetta, T.C. Hutchinson, H.B. Mason, J.D. Zupan, J.D. Bray , C. Bolisetti, A.S. Whittaker, Z.  
570 Chen, B.L. Kutter, Centrifuge modeling of structure-soil-structure interaction: Seismic performance of  
571 inelastic building models in: 15th World Conference on Earthquake Engineering, Lisbon, Portugal, 2012.

572 [29] H.B. Mason, N.W. Trombett, Z. Chen, J.D. Bray, T.C. Hutchinson, B.L. Kutter, Seismic soil–foundation–  
573 structure interaction observed in geotechnical centrifuge experiments Soil Dynamics and Earthquake  
574 Engineering, 48 (2013).

575 [30] J.A. Knappett, P. Madden, K. Caucis, Seismic structure–soil–structure interaction between pairs of  
576 adjacent building structures, Geotechnique, 65 (2015) 429–441.

577 [31] P. Cacciola, A. Tombari, Vibrating barrier: a novel device for the passive control of structures under  
578 ground motion, Proceedings of the Royal Society of London A: Mathematical, Physical and Engineering  
579 Sciences, 471 (2015).

580 [32] P Cacciola, M. Espinosaa, A. Tombari, Vibration control of piled-structures through structure-soil-  
581 structure-interaction, Soil Dynamics and Earthquake Engineering, 77 (2015) 47–57.

582 [33] L. Schwan, C. Boutin, L.A. Padron, M.S. Dietz, P.-Y. Bard and C. Taylor, Site-city interaction:  
583 theoretical, numerical and experimental crossed-analysis , Geophysical Journal International (2016) 205,  
584 1006–1031.

585 [34] C.B. J. Soubestre, M. Dietz, L. Dighoru, S. Hans, E. Ibrahim, C. A. Taylor, Dynamic Behaviour of  
586 Reinforced Soils -Theoretical Modelling and Shaking Table Experiments, *Geotechnical, Geological, and*  
587 *Earthquake Engineering* 22 (2012) 247-263.

588 [35] S. Bhattacharya, D. Lombardi, D.M. Wood, Similitude relationships for physical modelling of monopile-  
589 supported offshore wind turbines, *International Journal of Physical Modelling in Geotechnics*, 11 (2011) 58–  
590 68.

591 [36] A. S. Veletsos, and V. V. Nair, Seismic interaction of structures on hysteretic foundations, *Journal of*  
592 *Structural Engineering*, 101 (1975), 109-129.

593 [37] J. Bielak, Dynamic behaviour of structures with embedded foundations, *Earthquake Engineering &*  
594 *Structural Dynamics*, 3 (1974) 259-274.

595 [38] BS EN 1998-1:2004 Eurocode 8: Design of structures for earthquake resistance. Part 1: General rules,  
596 seismic actions and rules for buildings, in, European Committee for Standardization 2004.

597 [39] NEHRP Recommended Provisions for Seismic Regulations for New Buildings and Other Structures, Part  
598 1. FEMA 450, Chapter 3, pp 17-49, in, 2003.

599 [40] SEAOC Blue Book: Recommended Lateral Force Requirements and Commentary, 7 ed., Structural  
600 Engineers Association of California (SEAOC), 1999.

601 [41] D.D. Barkan Dynamics of bases and foundations, McGraw Hill Co., New York (1962).

602 [42] N. M. Newmark, E. Rosenblueth, Fundamentals of earthquake engineering, Prentice-Hall., 1971.

603 [43] C.F. Beards, Structural Vibration: Analysis and Damping, Arnold, 1996.

604 [44] PLAXIS 2D Geotechnical Software, in, Delft University of Technology and PLAXIS BV, 2012.

605 [45] A.J. Crewe, The Characterisation and Optimization of Earthquake Shaking Table Performance, in: Civil  
606 Engineering, University of Bristol, Bristol, 1998.

607 [46] S. Bhattacharya, A.M. Krishna, D. Lombardi, A. Crewe, N.A. Alexander, Economic MEMS based 3-axis  
608 water proof accelerometer for dynamic geo-engineering applications, *Soil Dynamics and Earthquake*  
609 *Engineering*, 36 (2012) 111–118

610 [47] MATLAB 7.6.0.324 (R2008a). Natick, Massachusetts: The MathWorks Inc. , in.

611 [48] PEER Strong Motion Database, in, The Pacific Earthquake Engineering Center and the University of  
612 California, 2000.

613 [49] J.F. Kenney, E.S. Keeping, Mathematics of statistics. Pt. 1, 3 ed., Van Nostrand, Princeton, NJ, 1962.

614

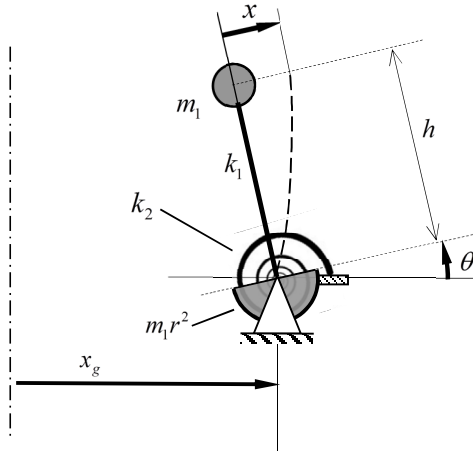


**Figure 21** Idealised two degree of freedom model.

Assuming linear elasticity and small angles, the Lagrangian (kinetic minus potential energy) of the above system is

$$\Pi = \frac{1}{2} m_1 (\dot{x} + \dot{x}_g - h\dot{\theta})^2 + \frac{1}{2} m_2 r^2 \dot{\theta}^2 - \frac{1}{2} k_1 x^2 - \frac{1}{2} k_2 \theta^2 \quad (8)$$

where  $m_1$  and  $k_1$  are the building's mass and stiffness respectively,  $m_2 r^2$  and  $k_2$  are the foundation/soil's rotational mass and stiffness respectively,  $r$  is the radius of gyration of the foundation/soil mass and  $h$  is the building height. Hence the Euler-Lagrange equations of motion are

$$m_1 (\ddot{x} + \ddot{x}_g - h\ddot{\theta}) + k_1 x = 0, \quad m_2 r^2 \ddot{\theta} - h m_1 (\ddot{x} + \ddot{x}_g - h\ddot{\theta}) + k_2 \theta = 0 \quad (9)$$

By introducing the following parameters

$$\alpha = \frac{m_2}{m_1}, \quad \eta = \frac{h}{r}, \quad \Omega = \frac{\omega_2}{\omega_1}, \quad \omega_1^2 = \frac{k_1}{m_1}, \quad \omega_2^2 = \frac{k_2}{m_2 r^2} \quad (10)$$

and non-dimensional variables,

$$x = ru, \quad x_g = ru_g, \quad t = \frac{\tau}{\omega_1} \quad (11)$$

where  $\tau$  is scaled time,  $u$  is scaled relative displacement and  $u_g$  is scaled ground displacement we can therefore re-expresses the Euler-Lagrange equations of motion, equation (9), in a dimensionless form as follows

$$\begin{bmatrix} 1 & -\eta \\ -\eta & \alpha + \eta^2 \end{bmatrix} \begin{bmatrix} u'' \\ \theta'' \end{bmatrix} + \begin{bmatrix} 1 & 0 \\ 0 & \alpha \Omega^2 \end{bmatrix} \begin{bmatrix} u \\ \theta \end{bmatrix} = \begin{bmatrix} -1 \\ \eta \end{bmatrix} u_g'' \quad (12)$$

where primes indicate derivatives with respect to scaled time  $\bullet'' = \partial^2 \bullet / \partial \tau^2$ . Hence the system reduces to one containing just three non-dimensional parameters: (i) a mass ratio  $\alpha$  (ii) an aspect ratio  $\eta$  and (iii) a frequency ratio  $\Omega$ .

The flexible-base fundamental natural circular frequency  $\omega_{f1}$  of the above system can be determined by solving the resultant homogenous eigenvalue problem. Hence the ratio of flexible-base  $\omega_{f1}$  to fixed-base  $\omega_1$  fundamental natural circular frequencies  $\Omega_f$  can be stated as follows

$$\Omega_f^2 = \frac{\omega_{f1}^2}{\omega_1^2} = \frac{1}{2} \left( \Omega^2 + 1 + \frac{\eta^2}{\alpha} - \frac{1}{\alpha} \sqrt{\alpha^2 \Omega^4 - 2\alpha^2 \Omega^2 + 2\alpha \Omega^2 \eta^2 + \alpha^2 + 2\alpha \eta^2 + \eta^4} \right) \quad (13)$$